Transition-metal profiles in a multicrystalline silicon ingot

Daniel Macdonald[a] and Andrés Cuevas
Department of Engineering, Faculty of Engineering and Information Technology, The Australian National University, Canberra, ACT 0200, Australia

A. Kinomura
National Institute of Advanced Industrial Science and Technology (AIST), 1-1-1 Umezono, Tsukuba, Ibaraki 305-8568, Japan

Y. Nakano
Kyoto University Research Reactor Institute, Kumatori-cho, Sennan-gun, Osaka 590-0494, Japan

L. J. Geerligs
Energy Research Center of the Netherlands (ECN) Solar Energy, P.O. Box 1, NL-1755 ZG Petten, The Netherlands

(Received 8 October 2004; accepted 8 November 2004; published online 19 January 2005)

The concentrations of transition-metal impurities in a photovoltaic-grade multicrystalline silicon ingot have been measured by neutron activation analysis. The results show that the concentrations of Fe, Co, and Cu are determined by segregation from the liquid-to-solid phase in the central regions of the ingot. This produces high concentrations near the top of the ingot, which subsequently diffuse back into the ingot during cooling. The extent of this back diffusion is shown to correlate to the diffusivity of the impurities. Near the bottom, the concentrations are higher again due to solid-state diffusion from the crucible after crystallization has occurred. Measurement of the interstitial Fe concentration along the ingot shows that the vast majority of the Fe is precipitated during ingot growth. Further analysis suggests that this precipitation occurs mostly through segregation to extrinsic defects at high temperature rather than through solubility-limit-driven precipitation during ingot cooling. © *2005 American Institute of Physics*. [DOI: 10.1063/1.1845584]

I. INTRODUCTION

Transition-metal impurities are detrimental to crystalline silicon solar cells, but are relatively common in photovoltaic-grade materials. They cause reduced solar cell conversion efficiencies through increased carrier recombination, whether they are present as isolated pointlike impurities or as precipitates. The purpose of this work is to study the concentration profiles of some common metallic impurities along the length of a standard directionally solidified multicrystalline silicon ingot grown for solar cell production.

The concentrations of such impurities are generally below 10^{15} cm^{-3}, and as such cannot be detected by physical techniques such as secondary-ion-mass spectroscopy. Deep-level transient spectroscopy and other electrical techniques are sensitive enough, but fail to give quantitative information on how many atoms are incorporated in precipitates. Here we have used neutron activation analysis (NAA), a technique which has been successfully applied to such material in the past,[1,2] to reveal the total concentrations of Fe, Co, Cu, Ag, Au, Zn, and Cr. The resulting concentration profiles are modeled using a simple segregation model, which explains the data well in regions which are not influenced by further diffusion of impurities after crystallization is complete.

NAA data do not provide any information regarding the chemical state of the impurities—they may be present as pointlike impurities or as precipitates. For the case of Fe we have also determined the concentration of electrically active interstitial Fe atoms via carrier lifetime measurements before and after dissociation of iron–boron pairs. The results reveal that the vast majority of the Fe must be precipitated, although both the interstitial and precipitated Fe concentrations have a similar shape along the ingot length. This latter fact suggests that the precipitation is chiefly driven by energetically favored segregation to extrinsic defects at high temperature, rather than the deceasing solubility limit during cooling. This in turn has implications for the chemical form of the precipitates and their behavior during solar cell processing.

II. EXPERIMENTAL METHODS

The multicrystalline ingot analyzed was a standard, boron-doped (nominally 1 Ω cm) ingot from a commercial process for solar cell production. Crystallization occurred from bottom to top, resulting in a vertical, columnar grain structure. The large square-based ingots are then sawn vertically into "bricks," which are in turn sawn horizontally into 12.5×12.5 cm^2 wafers for solar cell processing. Typically, thin slabs from the top and the bottom of the bricks are removed before wafering, as these sections have high impurity concentrations due to solid-state diffusion from the crucible at the bottom and from the impurity segregation at the top. In this case, however, the bottom and top sections were retained in order to monitor the entire vertical impurity profile.

The chosen brick was taken from the center of the ingot in order to avoid contamination from the crucible walls,

[a]Electronic mail: daniel.macdonald@anu.edu.au

which may extend over a few centimeters.[3,4] In addition, all measurements were performed on wafer sections that were vertically aligned, meaning that cross sections of the same columnar grains were included. This should minimize the impact of lateral variations in the metal content of the ingot.

A. Neutron activation analysis

Wafers for NAA were selected at 4%, 10%, 20%, 42%, and 98% of the total ingot length, as measured from the top, with the total ingot height being approximately 350 mm. A small section, approximately 8 cm^2 of each 300-μm-thick wafer, was subjected to NAA, giving a sample volume of around 0.25 cm^3. The analyzed wafer area is large enough to include a representative average of grain boundaries and intragrain regions, which is important considering that metal precipitates occur much more frequently at grain boundaries.[1,5]

Prior to NAA, the wafer sections were cut, chemically cleaned, and then etched in a HF/HNO_3 solution to a depth of approximately 15 μm per side to remove saw damage and surface contamination. The wafers were then chemically cleaned again in fresh solutions to minimize possible replating of dissolved impurities.

The samples were then subject to neutron activation for 190 h during 3 weeks with a nominal thermal-neutron flux of 4.7×10^{13} $n/cm^2\,s$ at the Research Reactor Institute, Kyoto University. The resulting gamma rays emitted by the decaying nuclei were monitored by a pure Ge detector, firstly for 1 h after a cooling time of about 4 days, then again for 24 h after 1 month. The measurement was, in principle, based on the monostandard method[6] using ^{197}Au as a single standard. The sensitivities of Ag, Co, Zn, Cu, and Fe were calibrated in advance by using samples with known concentrations of the relevant isotopes. These standard samples were prepared by ion implantation into Si wafers for the first five elements and by deposition of a thin metallic film on Si for the case of Fe (since the relevant isotope ^{58}Fe has a natural abundance of only 0.3%). As a result, the uncertainty in the NAA measurements was substantially improved, as indicated by the error bars in Figs. 2 and 3.

B. Interstitial iron measurements

To supplement the NAA results, the concentration of interstitial Fe (Fe_i), as opposed to the total Fe concentration, was measured on wafers from the same brick. This was achieved using a technique based on the optical dissociation of FeB pairs, which causes a characteristic change in the carrier diffusion length or lifetime.[7,8] This technique was originally developed for use with surface photovoltage (SPV) diffusion length measurements in low injection,[7] but has recently been extended to arbitrary injection,[8] meaning other lifetime measurement techniques can be used.

In this work, injection-dependent carrier lifetimes were measured using the quasisteady-state photoconductance (QSSPC) technique,[9] and values were extracted at an excess carrier concentration of 10^{15} cm^{-3}. Knowledge of the change in lifetime after FeB pair dissociation by illumination at this excess carrier density, coupled with the dopant concentration, allows very sensitive determination of the concentration of Fe_i.[8] A further benefit of measuring the injection dependence of the carrier lifetimes is that it provides independent confirmation that the changes due to illumination are indeed caused by Fe_i, as opposed to other possible light-induced changes, such as charging of the nitride layer,[10] boron–oxygen complexes,[11] or breaking of Cu_s–Cu_i pairs.[12] It has been shown that, for the case of Fe_i and FeB pairs, such injection-dependent lifetime curves display a characteristic "crossover" point at an excess carrier density between 1×10^{14} and 2×10^{14} cm^{-3}. We observed the presence of this crossover point in all the samples studied here.

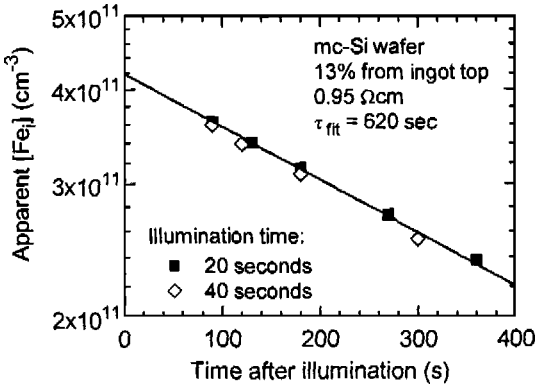

FIG. 1. Reduction in the "apparent" Fe_i concentration due to repairing after illumination. The straight line shows the exponential fit used to estimate $[Fe_i]$ immediately after illumination. Illumination times of 20 and 40 s are shown.

Surface passivation was achieved by plasma-enhanced chemical-vapor deposition of SiN films on both wafer surfaces after etching and cleaning.[13] The QSSPC technique measures an area of several square centimeters and thus provides an "average" of the Fe_i concentration across several grains. This can cause an overestimation (by up to a factor of 2) of $[Fe_i]$ if the lifetime varies considerably between grains.[8] Nevertheless, this error is small in comparison to the changes in $[Fe_i]$ observed along the ingot length.

It is essential that almost complete pairing and dissociation are ensured for the two measurements to enable the *total* Fe_i concentration to be determined. Initial measurements with the Fe_i in the paired state were performed after at least 3 h of repairing in the dark. For 1 Ω cm material this ensures more than 98% pairing. In this study, the illumination used to break the FeB pairs was white light with an intensity of approximately 0.7 W/cm^2 for a duration of 20 s. This is sufficiently intense to ensure a complete dissociation even in wafers with relatively low lifetimes.[14] The samples were clamped to a cooled Al block during illumination to minimize heating.

The slight delay between illumination and measurement allows some repairing, so several measurements were taken at varying time intervals to allow extrapolation to the initial state of almost complete dissociation. This is shown in Fig. 1 for a sample 13% from the top of the ingot. The total Fe_i concentration was determined to be 4.2×10^{11} cm^{-3}. The exponential fit gave a characteristic repairing time of 620 s. This value is within a factor of 2 of the expression from Zoth and Bergholz,[7] which gives a repairing time of 1100 s for

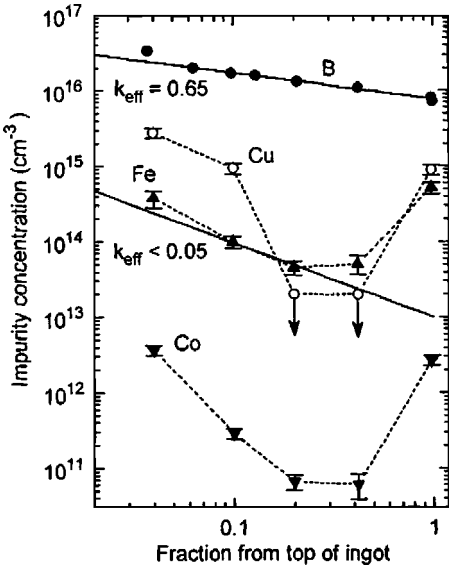

FIG. 2. Concentrations of B, Fe, Co, and Cu as a function of ingot position (fraction from top, hence 0 is the top, 1 the bottom). The straight lines are segregation model fits with $k_{\mathrm{eff}}=0.65$ for B and $k_{\mathrm{eff}}<0.05$ for Fe.

this 0.95 Ω cm sample at an assumed temperature of 35 °C. This fairly small disagreement will be the subject of a future publication. In Fig. 1, measurements for 20- and 40-s illuminations are shown to give the same result, indicating that the dissociation process was complete in both cases.

III. NAA RESULTS AND DISCUSSION

The NAA results for Fe, Co, and Cu are shown in Fig. 2, as well as the boron concentration measured via the dark conductance of the wafers. The NAA results for Cr, Zn, Ag, and Au are plotted in Fig. 3. For all of these impurities, the measured concentrations are well below their respective solid solubility limits near the melting point of silicon.[15] Due to the qualitative difference between the profiles of the first set of metals and the second, they are discussed separately below.

A. NAA results for Fe, Co, and Cu

For Fe, Co, and Cu, the concentration profiles along the ingot length show similar trends. In the central regions of the ingot, their concentrations are low. There is a strong increase towards the top of the ingot due to segregation into the molten phase, while the sharp increase at the bottom is probably due to solid state in diffusion from the crucible after solidification. Considering that the bottom is the first part to crystallize, there is ample time at high temperature for this to occur (tens of hours, generally).

The concentration of impurities incorporated into the solid phase C_S during crystallization is given by $C_S=k_0C_l$ where k_0 is the equilibrium segregation coefficient and C_l is the concentration of impurities at the solid/liquid interface.[16] The value of C_l may be very different from the concentration in the bulk liquid C_L due to imperfect mixing. In such cases the effective segregation coefficient k_{eff} is used, $C_S=k_{\mathrm{eff}}C_L$, where k_{eff} depends on the growth rate v, the diffusivity of the impurities in the molten phase D, and the boundary layer thickness δ,

$$k_{\mathrm{eff}}=\frac{k_0}{k_0+(1-k_0)\exp(-v\delta/D)}. \tag{1}$$

The boundary layer thickness approximates the width of the region near the interface in which no convection or mixing currents occur. The critical point is whether or not the impurities are able to diffuse out of the static boundary layer and into the bulk melt before being overtaken by the advancing crystallization front.

Assuming a fixed volume of solidifying liquid, as is the case in multicrystalline silicon growth, gives rise to the Scheil equation,[17,18]

$$C_S=k_{\mathrm{eff}}C_0(1-f_s)^{k_{\mathrm{eff}}-1}, \tag{2}$$

where C_0 is the initial concentration in the liquid and f_S is the solidified fraction.

This expression describes the distribution of boron in the ingot quite well, as shown in Fig. 2, using $k_{\mathrm{eff}}=0.65$. This is a little lower than the literature value for k_0 of 0.8.[19] For effective segregation coefficients less than approximately 0.05, the *shape* of the impurity profile is indistinguishable, although for smaller values the *magnitude* is reduced for a given initial concentration in the melt. This reflects the fact that for low segregation coefficients, the shape of the profile is governed entirely by the almost complete ejection of impurities into a decreasing melt volume.

Figure 2 shows an attempt to fit the Scheil expression to the measured Fe concentration using $k_{\mathrm{eff}}<0.05$. In this case the data are distorted at the top and bottom by solid-state diffusion during postcrystallization cooling. Nevertheless, the model is in reasonable agreement with the upper part of the ingot. The equilibrium segregation coefficient for Fe is reported[20,21] as $k_0=(5-7)\times10^{-6}$. This would imply an initial concentration of Fe in the melt of 2×10^{18} cm^{-3}. This is extremely unlikely and may be explained by the incomplete mixing in the molten phase, producing a much larger segregation coefficient than the equilibrium value. It is also possible that the effective segregation coefficient is increased by the rapid precipitation of Fe at extended defects during crystallization, as discussed in Sec. IV.

Applying the Scheil equation with $k_{\mathrm{eff}}<0.05$ to the data for Co and Cu results in a poorer fit. Although they show the

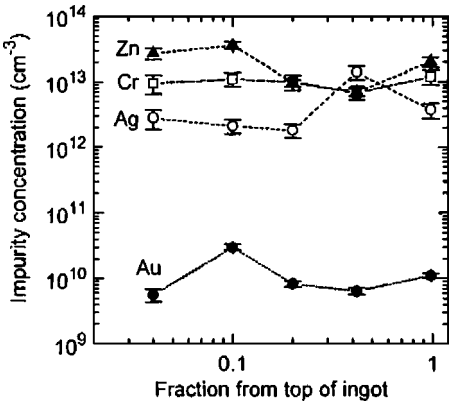

FIG. 3. Concentrations of Au, Ag, Cr, and Zn as a function of ingot position (fraction from top).

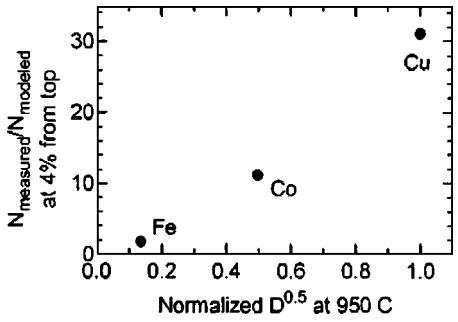

FIG. 4. Ratio of measured to modeled impurity concentrations for Fe, Co, and Cu, as a function of $D^{0.5}$ at 950 °C, the normalized, approximate diffusion length for these impurities at the top of the ingot during cooling.

same trend as for Fe, i.e., they increase towards the top, this increase is much greater than is possible with the Scheil equation. This deviation may be due to solid-state diffusion back into the ingot after crystallization is complete.

The extent of this back diffusion will be determined by the diffusion length of the respective impurities during cooling. This is in turn will be determined by the cooling rate and the diffusivity at each temperature. Since the cooling rate is not well known in this case, nor are the diffusivities known for the whole temperature range, it is difficult to model this back diffusion accurately.

Nevertheless, a simple evaluation is instructive. The Scheil equation with $k_{\text{eff}} < 0.05$ was fitted to the lowest measured data point for each impurity. The ratio of the *measured* concentration to this modeled curve was then determined at 4% below the top of the ingot. This should approximately represent the extent of back diffusion. The results are plotted in Fig. 4 against the normalized square root of the diffusivity for Fe, Co, and Cu in silicon at 950 °C (a temperature at which the diffusivity is known for all three[15]). While this does not provide a precise simulation of the back-diffusion process, the figure nevertheless shows a clear correlation between the extent of back diffusion and the diffusivity for each impurity. This clearly indicates that the deviation from the segregation model near the top of the ingot is due to solid-state back diffusion. In the case of Cu, Fig. 2 shows that the back diffusion extends more than 10% of the ingot height, a distance of more than 3 cm. As an order-of-magnitude approximation for the cooling period, the diffusion length[15] of Cu in silicon at 1000 °C for 10 h is around 2 cm, in approximate agreement.

B. NAA results for Cr, Zn, Ag, and Au

Figure 3 shows the NAA results for Cr, Zn, Ag, and Au. They show relatively flat profiles and lack the characteristic increase at the bottom and at the top of the ingot due to postcrystallization contamination and segregation. In all cases the NAA spectra were clearly identified, and the uncertainties in each measurement are quite small, being much less than the apparently random fluctuations in the data. This suggests the possibility of surface contamination. Contamination levels in the range of 10^{10}–10^{11} cm^{-2} would be sufficient for Ag, Cr, and Zn, while values as low as 10^{8} cm^{-2} are all that is required for the amount of Au detected.

However, it is worth considering if such flat profiles can possibly occur through segregation for metals with very small equilibrium segregation coefficients ($k_0 < 0.0001$ for each of these metals[20,21]). Firstly, in relation to the lack of concentration peaks at the bottom of the ingot, in diffusion from the crucible would not actually be expected for Zn, Ag, and Au, since they have much lower diffusivities in the solid state than Fe, Co, or Cu. This is due to the fact that they diffuse via the kick-out mechanism.[15,22] Cr, however, diffuses interstitially, and its diffusivity is only a little lower than that of Fe. Hence some in diffusion of Cr from the crucible would be expected if it were present there in high enough concentrations.

Regarding the flat profiles throughout the rest of the ingot, this would require k_{eff} values close to unity. According to Eq. (1), this can occur through changes in the values of the growth rate, the boundary layer thickness, or the diffusivity of the impurities in the melt. Since the first two must be the same for all species, only the changes in the diffusivity can increase k_{eff} for some impurities relative to others. However, modeling using Eqs. (1) and (2), with realistic growth rates in the range of 2–20 μm/s,[23] reveals that this would require a diffusivity for Cr, Au, Ag, and Zn of at least an order of magnitude smaller than that for Fe, Co, and Cu. This seems unlikely, since the diffusivities of different impurities in molten silicon are quite similar despite enormous differences in the solid state.[19,24] For example, impurities as diverse as B, P, Al, O, C, Fe, and Cu have diffusivities in molten silicon[19,24] that fall within the range of $(0.5–7)\times 10^{-4}$ cm^2 s^{-1} (for Fe and Cu a value of 2×10^{-4} cm^2 s^{-1} has been suggested[24]). Although values are not known for Cr, Zn, Ag, or Au, they would probably also fall within this range.

In conclusion then, although it is not possible to definitely rule out the profiles for Cr, Zn, Ag, and Au reflecting concentrations in the bulk of the wafers, it seems that the most likely explanation is surface contamination. Such surface contamination has been reported for Cr via replating of the metal onto the silicon surface during wet processing.[15] It is worth bearing in mind that the lower values for Fe, Co, and Cu may also be affected by surface contamination. This may be the reason for the slightly higher measured values for Fe and Co at 40% from the ingot top, where solid-state diffusion should not occur, in comparison to the Scheil equation fit.

IV. TOTAL AND INTERSTITIAL IRON RESULTS

For the case of Fe it is possible to compare the total Fe concentration [Fe] as measured by NAA to the interstitial Fe concentration [Fe$_i$] from the lifetime measurements before and after dissociation of the FeB pairs. The results are shown in Fig. 5. The data for the interstitial Fe concentration are not available at the very top and bottom of the ingot because the carrier lifetimes there are too low to allow a complete FeB pair dissociation.

The striking feature is that the interstitial Fe data also follow the Scheil equation, apart from a deviation near the top of the ingot, presumably due once again to solid-state back diffusion. These data are in qualitative agreement with

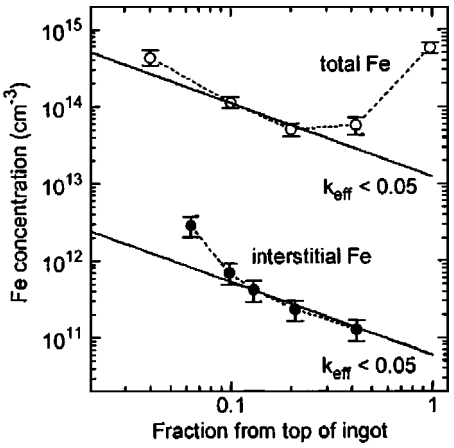

FIG. 5. Concentrations of total Fe and interstitial Fe as a function of ingot position (fraction from top). The straight lines are segregation model fits with $k_{\text{eff}} < 0.05$.

recently published results for similar multicrystalline ingots using the same Fe_i detection technique.[25,26] Another observation is that the vast majority of the Fe is not in interstitial form and must therefore be present as precipitates. The results presented here allow some speculation as to how these precipitates form.

Since Fe only precipitates heterogeneously[15] (unlike Cu or Co), the precipitates must form at extrinsic defects in the material such as grain boundaries and dislocations. There are two distinct mechanisms which can influence the amount of precipitated Fe at a given point in the ingot after cooling. These have been referred to as "relaxation" and "segregation" gettering,[27,28] the latter word is a reference to the fact that the extrinsic defects act as internal gettering sites. These two mechanisms are discussed in turn in relation to our measurements.

A. Relaxation mechanism

In the relaxation process the precipitation is driven by the decreasing solid solubility limit during the cooling of the ingot. Just below the melting point of Si, the solubility[15] of Fe is above 10^{16} cm^{-3}, well above any of the measured values here. Hence all of the Fe is initially dissolved in the solid state. As the ingot cools after crystallization is complete, the solubility limit also decreases until it reaches the local Fe concentration. If the excess Fe atoms are still diffusive enough, they can reach extrinsic defects and precipitate. Eventually, the diffusivity becomes too low and the remaining nonprecipitated Fe is frozen in the interstitial state. The determining factors for the final concentration of interstitial Fe under the relaxation process are then the *cooling rate* and the *density of extrinsic defects*. If these are the same everywhere in an ingot, then the final value of $[Fe_i]$ should be constant, irrespective of variations in the initial Fe content.

Recent numerical simulations[29] of multicrystalline silicon ingot growth have shown that most parts of an ingot cool at approximately the same rate below 1200 °C (at which temperature the solubility of Fe is still above 10^{16} cm^{-3}), except for the very top, bottom, and edges. Similarly, the density of extrinsic defects, the most important of which are probably grain boundaries and dislocations, also increases near the very top, bottom, and edges, but is generally fairly constant throughout the central regions. It therefore seems unlikely that the relaxation mechanism explains the observed $[Fe_i]$ trend in the central region. According to the relaxation model and assuming an effective segregation coefficient k_{eff} similar to the equilibrium value[20,21] of $k_0 = (5-7) \times 10^{-6}$, then the starting concentration of Fe in the melt would be as high as 2×10^{18} cm^{-3}, which is also unlikely.

B. Segregation mechanism

The fact that the two sets of Fe profiles are observed to be parallel hints that maybe the concentration of interstitial Fe is actually formed at higher temperatures, rather than during the cool down. This can occur via the so-called segregation mechanism, in which there is not only segregation from the liquid melt to the bulk solid, but also to extrinsic defects within the solid. The precise mechanism of the segregation to extrinsic defects is unclear—it may occur either directly from the liquid phase or after a brief incorporation in the bulk solid. In either case, the system can be thought of as equilibrium segregation occurring between *three* phases (the third phase being the extrinsic defects), rather than just two. Segregation to extrinsic defects is driven by lower free energies for metal atoms where the lattice is distorted, as compared to regions of perfect crystal structure.[27,28] Note that this implies that precipitation can proceed even when the dissolved concentration is well below the solubility limit. This phenomenon has been observed recently for Fe in defected silicon.[27,28]

Consider the case when the crystallization occurs slowly enough to allow the three-phase segregation processes to equilibrate. Assume also that segregation to the extended defects occurs primarily from the solid phase, rather than directly from the liquid phase. Given that typical crystallization velocities are in the range of $5-10$ μm/s in the central part of the ingot,[23] and that the diffusion length of Fe atoms in the solid phase near the melting point is around 30 μm in a time of 1 s, then equilibration will occur in regions where the average distance between extrinsic defects is of a similar distance (30 μm) or less. For dislocations, this corresponds to an areal dislocation density of approximately 10^5 cm^{-2}.

Multicrystalline silicon materials commonly have numerous regions with dislocation densities above 10^6 cm^{-2}.[30,31] Hence it is likely that in such regions the segregation of Fe to extrinsic defects will deplete the Fe concentration in the solid phase near the interface, resulting in greater incorporation from the liquid phase, and hence a larger effective segregation coefficient. On the other hand, if the distance between extrinsic defects is large, the segregation process will not occur until some time after the crystallization front has passed and will not result in increased incorporation from the melt. This implies that the total Fe concentration in highly dislocated regions would be much higher than that in other parts of an ingot.

The starting concentration of Fe in the melt can be estimated within the framework of this segregation mechanism. Assume that in highly dislocated regions the three phases are

in equilibrium, and therefore there is increased segregation from the melt in those regions. If we also assume that the Fe precipitated in this way dominates the total Fe concentration, then the relevant concentration in the solid phase for determining the starting concentration in the melt is the *interstitial* concentration, rather than the *total* concentration. Assuming an effective segregation coefficient k_{eff} similar to the equilibrium value[20,21] of $k_0=(5-7)10^{-6}$, the starting concentration of Fe in the melt would then be around 1×10^{16} cm^{-3}, compared with 2×10^{18} cm^{-3} for the relaxation mechanism. This seems a more reasonable value, although it may still be too high considering that incomplete mixing in the melt may increase the effective segregation coefficient from its equilibrium value. If such a high starting concentration did occur, it is unlikely to come solely from the starting polysilicon material, suggesting contamination from handling or from the crucible during the melting stage.

Reflecting these processes mathematically, it is possible to express the effective segregation coefficient between liquid and solid (excluding precipitated atoms), $k_{\text{eff}}=C_S/C_L$, in terms of segregation coefficients between the liquid phase and extrinsic defects, $k_{L/\text{ED}}$, and between extended defects and the bulk solid phase, $k_{\text{ED}/S}$, such that $k_{\text{eff}}=k_{L/S}=k_{L/\text{ED}}k_{\text{ED}/S}$. This model naturally leads to a situation where the interstitial and dissolved Fe concentrations both follow segregation-model curves, as observed in Fig. 5. Furthermore, the data in Fig. 5 allow us to estimate $k_{\text{ED}/S}\approx0.005$. If we assume that $k_{\text{eff}}=k_{L/S}$ is approximately equal to the equilibrium value k_0 from the literature, this implies that $k_{L/\text{ED}}\approx0.001$. This value is below 0.05, for which different curves are indistinguishable in shape in a plot such as Fig. 5. This is in agreement with the observation that the total Fe curve does indeed follow the Scheil equation with $k_{\text{eff}}<0.05$.

The results suggest that the precipitated and interstitial Fe concentrations as formed at high temperatures are largely preserved during the cooling down of the ingot. This could occur if $k_{\text{ED}/S}$ itself is relatively temperature independent, or if there are kinetic barriers against further precipitation or dissolution of Fe.

It is instructive to note that the ratio of interstitial to total Fe concentration, or in other words $k_{\text{ED}/S}$, is quite constant in the central regions of the ingot. This is consistent with the fact that the density of extrinsic defects is roughly constant in this region. This value may increase significantly towards the edges and ends of the ingot due to an increase in the extrinsic defect concentration. It could also vary considerably for different growth processes. In recent experiments with segregation of Fe from monocrystalline silicon to a thin film of polycrystalline silicon (at temperatures between 1050 and 1200 °C), Istratov *et al.* found values for $k_{\text{ED}/S}$ of 0.06 and 0.4.[27]

C. Relative importance of the two mechanisms

It is likely that in grains with high densities of dislocations, above approximately 10^5 cm^{-2}, the segregation mechanism would be dominant and may act quickly enough to allow depletion of the solid phase near the interface, and hence result in increased incorporation into the solid phase. This would also occur if segregation to extended defects proceeded directly from the melt, rather than via the solid phase.

However, in large grains of high crystal quality, with sparsely distributed extrinsic defects, such depletion near the liquid/solid interface will not occur. In these regions, segregation precipitation will proceed on a slower time scale determined by the extrinsic defect density. In such regions the relaxation mechanism may also play an important role in the precipitation. It is therefore possible that there is a mixture of both segregation and relaxation precipitation occurring during ingot growth. However, the fact that both the interstitial and precipitated Fe profiles are parallel suggests that the segregation mechanism is responsible for the vast majority of the Fe precipitation.

A further consequence of the segregation versus relaxation mechanism relates to the chemical form of the precipitates. Since under the segregation mechanism the precipitates are created at relatively high temperatures, just below the melting point, they are probably mostly in the form of α-$FeSi_2$, which forms above approximately 920 °C.[32] These silicides have large binding energies and are very difficult to dissolve during subsequent solar cell processing. This may explain the observation that highly dislocated regions do not respond well to phosphorus gettering.[30,31] On the other hand, for the relaxation precipitation mechanism, a significant proportion may occur as β-$FeSi_2$, which are formed[33] below 800 °C and therefore more easily dissolved and removed by gettering.

V. CONCLUSIONS

The total concentrations of Fe, Co, and Cu along the length of a photovoltaic-grade multicrystalline silicon ingot appear to be determined by segregation from the liquid to the solid phase in the central region of the ingot. Near the bottom the concentrations are higher due to in diffusion in the solid state from the crucible. Near the top, the segregated impurities diffuse back into the solid ingot during cooling. The extent of this back diffusion is clearly related to the diffusivity of each impurity. For Cu, the back diffusion extends over several centimeters. Maximum concentrations of 3.8×10^{14}, 3.7×10^{12}, and 2.8×10^{15} cm^{-3} were detected near the top of the ingot for Fe, Co, and Cu, respectively.

For the case of Fe, the interstitial Fe concentration was measured in addition to the total Fe concentration. The results indicate that only approximately 1 in 200 Fe atoms occur interstitially. However, the two profiles followed similar curves, indicating that the majority of the Fe precipitation is driven by energetically favored segregation to extrinsic defects at high temperature, rather than by the decreasing solubility limit during ingot cooling.

ACKNOWLEDGMENTS

The authors are grateful to J. S. Williams for coordinating the joint research between ANU and AIST, and to T. Buonassisi for enlightening discussions. This work has been carried out in part under the Visiting Researcher's Program of the Kyoto University Research Reactor Institute. One of the authors (L.J.G.) acknowledges the assistance of The

Netherlands Agency for Energy and the Environment. Two of the authors (D.M. and A.C.) acknowledge the support of the Australian Research Council.

[1]A. A. Istratov, T. Buonassisi, R. J. McDonald, A. R. Smith, R. Schindler, J. A. Rand, J. P. Kalejs, and E. R. Weber, J. Appl. Phys. **94**, 6552 (2003).
[2]D. Macdonald, A. Cuevas, A. Kinomura, and Y. Nakano, in *Proceedings of the 29th IEEE Photovoltaic Specialists Conference*, New Orleans, LA, (IEEE, New York, 2002), p. 285.
[3]M. Acciarri, S. Binetti, S. Ratti, C. Savigni, S. Pizzini, F. Ferrazza, and D. Margadonna, in *Proceedings of the 13th European Photovoltaic Solar Energy Conference*, Nice, France, (HS Stephens and Associates, Felmersham, UK, 1995), p. 1336.
[4]M. Rinio, C. Ballif, T. Buonassisi, and D. Borchert, in Proceedings of the 19th European Photovoltaic Solar Energy Conference, Paris, 2004 (to be published).
[5]S. A. McHugo *et al.*, J. Appl. Phys. **89**, 4282 (2001).
[6]J. I. Kim, J. Radioanal. Chem. **63**, 121 (1981).
[7]G. Zoth and W. Bergholz, J. Appl. Phys. **67**, 6764 (1990).
[8]D. Macdonald, L. J. Geerligs, and A. Azzizi, J. Appl. Phys. **95**, 1021 (2004).
[9]R. A. Sinton and A. Cuevas, Appl. Phys. Lett. **69**, 2510 (1996).
[10]A. G. Aberle, *Crystalline Silicon Solar Cells: Advanced Surface Passivation and Analysis* (University of New South Wales, Sydney, 1999).
[11]J. Schmidt and A. Cuevas, J. Appl. Phys. **86**, 3175 (1999).
[12]W. B. Henley, D. A. Ramappa, and L. Jastrezbski, Appl. Phys. Lett. **74**, 278 (1999).
[13]M. J. Kerr and A. Cuevas, Semicond. Sci. Technol. **17**, 166 (2002).
[14]L. J. Geerligs and D. Macdonald, Appl. Phys. Lett. (to be published).
[15]K. Graff, *Metal Impurities in Silicon-Device Fabrication*, Springer Series in Material Science (Springer, Berlin, 2000).
[16]J. R. Carruthers and A. F. Witt, in *Crystal Growth and Characterization*, edited by R. Ueda and J. B. Mullin (North-Holland, Amsterdam, 1975), p. 107.
[17]E. Scheil, Z. Metallkd. **34**, 70 (1942).
[18]R. A. Brown and D. H. Kim, J. Cryst. Growth **109**, 50 (1991).
[19]H. Kodera, Jpn. J. Appl. Phys. **2**, 212 (1963).
[20]J. R. Davis, A. Rohatgi, R. H. Hopkins, P. D. Blais, P. Rai-Choudhury, J. R. McCormick, and H. C. Mollenkopf, IEEE Trans. Electron Devices **27**, 677 (1980).
[21]H. Lemke, in *Semiconductor Silicon/1994*, edited by H. R. Huff, W. Bergholz, and K. Sumino (The Electrochemical Society, New Jersey, 1994), p. 695.
[22]D. Grünebaum, T. Czekalla, N. A. Stolwijk, H. Mehrer, I. Yonenaga, and K. Sumino, Appl. Phys. A: Solids Surf. **53**, 65 (1991).
[23]I. Steinbach, M. Apel, T. Rettelbach, and D. Franke, Sol. Energy Mater. Sol. Cells **72**, 59 (2002).
[24]G. F. Wakefield, J. Electrochem. Soc. **127**, 1139 (1980).
[25]R. A. Sinton, in Proceedings of the 19th European Photovoltaic Solar Energy Conversion Conference, Paris, 2004 (to be published).
[26]L. J. Geerligs, in Proceedings of the Third World Conference on Photovoltaic Solar Energy Conversion (WCPEC-3), Osaka, 2003 (unpublished), p. 1044.
[27]A. A. Istratov, T. Buonassisi, W. Huber, and E. R. Weber, in *Proceedings of the 14th Workshop on Crystalline Silicon Solar Cell Materials and Processes*, Winter Park, CO, (NREL, Golden, CO, 2004), p. 230.
[28]A. A. Istratov, W. Huber, and E. R. Weber, Appl. Phys. Lett. (submitted).
[29]D. Franke, T. Rettelbach, C. Häßler, W. Koch, and A. Müller, Sol. Energy Mater. Sol. Cells **72**, 83 (2002).
[30]B. L. Sopori, L. Jastrzebski, and T. Tan, in *Proceedings of the 25th IEEE Photovoltaic Specialists Conference*, Washington, DC, (IEEE, New York, 1996), p. 625.
[31]D. Macdonald, A. Cuevas, and F. Ferrazza, Solid-State Electron. **43**, 575 (1999).
[32]D. A. Ramappa and W. B. Henley, J. Electrochem. Soc. **144**, 4353 (1997).
[33]W. B. Henley and D. A. Ramappa, J. Appl. Phys. **82**, 589 (1997).